Journal of Cerebral Blood Flow & Metabolism (2015) 35, 312–318

www.jcbfm.com

ORIGINAL ARTICLE

Effect of age and vascular anatomy on blood flow in major cerebral vessels

Sepideh Amin-Hanjani[1], Xinjian Du[1], Dilip K Pandey[2], Keith R Thulborn[3] and Fady T Charbel[1]

Measurement of volume flow rates in major cerebral vessels can be used to evaluate the hemodynamic effects of cerebrovascular disease. However, both age and vascular anatomy can affect flow rates independent of disease. We prospectively evaluated 325 healthy adult volunteers using phase contrast quantitative magnetic resonance angiography to characterize these effects on cerebral vessel flow rates and establish clinically useful normative reference values. Flows were measured in the major intracranial and extracranial vessels. The cohort ranged from 18 to 84 years old, with 157 (48%) females. All individual vessel flows and total cerebral blood flow (TCBF) declined with age, at 2.6 mL/minute per year for TCBF. Basilar artery (BA) flow was significantly decreased in individuals with one or both fetal posterior cerebral arteries (PCAs). Internal carotid artery flows were significantly higher with a fetal PCA and decreased with a hypoplastic anterior cerebral artery. Indexing vessel flows to TCBF neutralized the age effect, but anatomic variations continued to impact indexed flow in the BA and internal carotid artery. Variability in normative flow ranges were reduced in distal vessels and by examining regional flows. Cerebral vessel flows are affected by age and cerebrovascular anatomy, which has important implications for interpretation of flows in the disease state.

Journal of Cerebral Blood Flow & Metabolism (2015) **35,** 312–318; doi:10.1038/jcbfm.2014.203; published online 12 November 2014

Keywords: cerebral blood flow; cerebral blood flow measurement; cerebrovascular disease; magnetic resonance; MR angiography

INTRODUCTION

Evaluation of blood flow is an important component of assessing patients with cerebrovascular disease. Cerebral blood flow (CBF) can be assessed with imaging techniques, which focus on evaluating regional CBF at the tissue level using modalities such as single positron emission tomography, xenon computed tomography, positron emission tomography, and computed tomography- or magnetic resonance (MR)-based perfusion imaging.[1] Alternatively, CBF can also be evaluated by examining the volume flow (in mL/minute) within the individual cerebral vessels supplying the brain tissue, using phase contrast quantitative magnetic resonance angiography (QMRA). Such flow rates have been used to assess a variety of cerebrovascular conditions including steno-occlusive diseases of the anterior and posterior circulation,[2] and the effects of interventions such as carotid endarterectomy, bypass surgery, and angioplasty/stenting.[3–7]

Reference values for the primary feeder vessels of the intracranial circulation, namely the basilar artery (BA) and internal carotid arteries (ICAs) have been previously reported,[8] but have not been reported for the primary vessels distal to the Circle of Willis. Furthermore, although variability in proximal vessel flows have been previously reported with respect to age and anatomic variations in the Circle of Willis,[9,10] these factors have not been assessed in a large cohort of healthy individuals spanning clinically relevant age ranges. In this study, we present the largest set of reference data in healthy subjects, examining the effect of both patient variables and vascular anatomy.

MATERIALS AND METHODS

Subjects

The study was approved by the University of Illinois at Chicago Institutional Review Board, and informed consent was obtained from all the study participants. The study was conducted under the general guidelines governing ethical research practices and protection of human research subjects in accordance with the code of federal regulations (CFR) Title 45 Part 46 of the US Department of Health and Human Services. From May 2004 to September 2013, 334 healthy subjects were prospectively enrolled. Adults >18 years old, with no history of cerebrovascular disease, were recruited. Patients were screened with regard to a history of cardiac or respiratory problems, stroke or seizures, liver or kidney disease, cancer, brain surgery, diabetes, or untreated hypertension, and excluded if they had any of these conditions or smoked greater than one pack of cigarettes per day. Pregnant women or those with contraindication to MRI were also excluded. Systolic and diastolic blood pressure was recorded before and after imaging; mean arterial pressure (MAP) was calculated and averaged over the two measurements for each patient. Patients ($n=9$) were excluded from data analysis if systolic blood pressure averaged $\geqslant 160$, leaving a total cohort of 325 patients.

Imaging

All the subjects underwent phase contrast QMRA performed on a 3.0 Tesla MRI Scanner (Signa VHi to HDx, General Electric Medical Systems, later GE Healthcare, Milwaukee, WI, USA) using either a four-channel or eight-channel neurovascular coil. The volume flow rate measurements were acquired with the Noninvasive Optimal Vessel Analysis software (VasSol, Chicago, IL, USA). This technique of flow measurement has been previously

[1]Department of Neurosurgery, University of Illinois at Chicago, Chicago, Illinois, USA; [2]Department of Neurology and Rehabilitation Medicine, University of Illinois at Chicago, Chicago, Illinois, USA and [3]Center for Magnetic Resonance Research, University of Illinois at Chicago, Chicago, Illinois, USA. Correspondence: Dr S Amin-Hanjani, Department of Neurosurgery, University of Illinois at Chicago, Neuropsychiatric Institute, Rm 451N, 912 S. Wood Street, M/C 799, Chicago, IL 60612, USA.
E-mail: hanjani@uic.edu
This study was supported by Dr Ralph and Marian Falk Research Trust Foundation.
Received 20 June 2014; revised 21 September 2014; accepted 16 October 2014; published online 12 November 2014

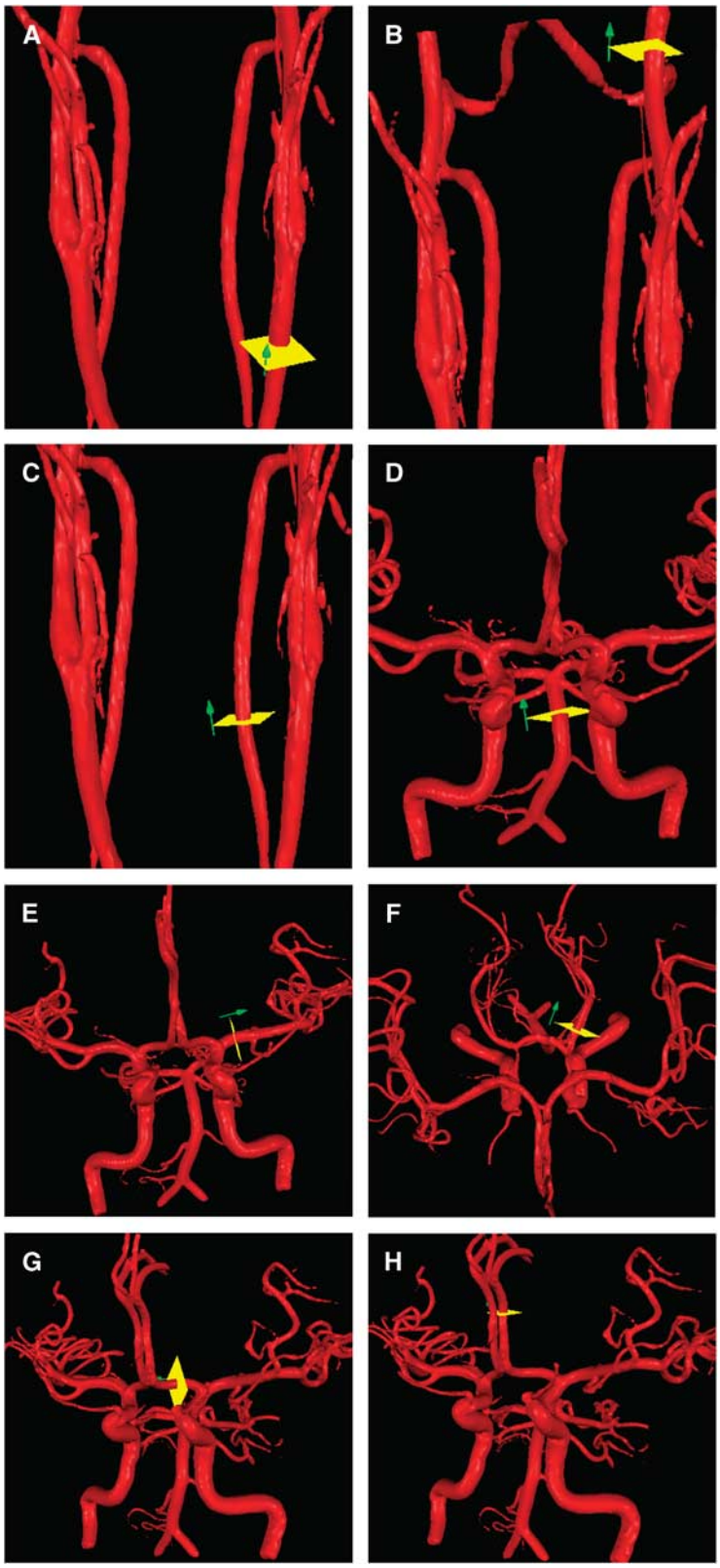

Figure 1. Location of flow measurements in the intracranial and cervical vasculature. (**A**) Common carotid artery. (**B**) Internal carotid artery. (**C**) Vertebral artery. (**D**) Basilar artery. (**E**) Middle cerebral artery. (**F**) Posterior cerebral artery. (**G**) Anterior cerebral artery pre-communicating segment (A1). (**H**) Anterior cerebral artery post-communicating segment (A2).

published,[11,12] and can be summarized as follows. The major extracranial arteries in the neck were first visualized by two-dimensional MRA time-of-flight (TOF) technique (TR/TE, 23 millisecond/4.6 millisecond; flip angle, 60°; FOV, 200 mm; slice thickness, 2 mm; matrix, 256/192; NEX, 1). Then, a three-dimensional MRA TOF of the head was obtained with parameters: TR/TE, 23/3.3 millisecond; flip angle, 20°; FOV, 220 mm; section thickness, 1 mm; matrix, 512 × 256. The MRA TOF images of the head and neck were sent to the Noninvasive Optimal Vessel Analysis software running on a separate workstation to reconstruct a three-dimensional surface-rendering of the vasculature used for automated determination of the double oblique scan plane perpendicular to flow of the vessels of interest. Volume flow measurements based on these planes at each vessel were performed using cardiac-gated phase contrast MR angiography (TR, 10 to 15 millisecond; TE, 4 to 7 millisecond; flip angle, 15°; NEX, 4; slice thickness, 3 mm for intracranial arteries and 5 mm for neck arteries; FOV, 140 mm for intracranial arteries and 180 mm for neck arteries; matrix, 256 × 192 for intracranial arteries and 256 × 128 for neck arteries). Velocity encoding was automatically verified by the Noninvasive Optimal Vessel Analysis software to ensure that aliasing did not occur for high velocities within the velocity range chosen for phase encoding of individual vessels. The selection of different velocity ranges for different vessels ensured maximum accuracy by using the full phase encoding range for each vessel. Volumetric flow rate (mL/minute) in each artery was processed by the Noninvasive Optimal Vessel Analysis software after phase contrast images had been acquired. The accuracy and precision of the protocol used in this study has been published previously.[12]

For all subjects, flows in the major intracranial and cervical arteries were measured in standard locations (Figure 1). These arteries consisted of the left (L) and right (R) common carotid artery, ICA, vertebral artery (VA), proximal middle cerebral artery (MCA), anterior cerebral artery (ACA) proximal pre-communicating segment (A1 segment), posterior cerebral artery (PCA), and BA. Total cerebral blood flow (TCBF) was calculated as the summation of bilateral VAs and ICAs. Given the well-recognized asymmetries in A1 and VA vessels, the sum of A1 and VA flow (designated as TACA and TVA, respectively) was calculated. Starting in June 2006, measurement on the ACA post-communicating segment (A2 segment) was also added to the imaging protocol, and was performed on 192 subjects. Regional flow to the L and R anterior circulation, termed L region (LR) and R region (RR), respectively, were calculated from the summation of ipsilateral MCA, PCA, and A2 flow. Posterior region (PR) flow was calculated from the sum of BA and PCA flows.

Subject vascular anatomy was determined based on the three-dimensional maximum intensity projection reconstructed maps of the TOF images. The A1 segment was designated as hypoplastic if measuring <15 mL/minute in flow. The PCA was designated as fetal if the P1 segment was absent/nonvisualized; the posterior communicating artery (PCoA) was designated as absent if not visualized or measurable.

Statistical Analysis

Quantitative volume flow rates are expressed as means ± s.d. Outliers were discarded if the data value was less than first quartile minus 1.5 times interquartile range or more than third quartile plus 1.5 times interquartile range. Sample normal distribution of each age group was identified by normal probability plot or Shapiro–Wilk test. Mean volumetric flow r ate values were calculated for each artery, TCBF, LR, RR, and PR; TCBF was examined relative to age using local regression models to identify appropriate age groupings.

Linear regression analysis was performed to assess the age and gender dependence of TCBF, LR, RR, and PR. One-way analysis of variance was used to estimate the significance of difference in flow among age groups. Similarly, the effect of race, gender, and MAP was examined. For paired vessels (MCA, A1 segment, A2 segment, PCA, VA), comparison of L and R flows were performed with paired *t*-test. *T*-test was performed to examine the differences in flows in the BA and ICAs relative to anatomic variations (fetal PCA, absent PCoA, and hypolastic A1 segment). All data analyses were performed using the statistical software package SAS (version 9.2, SAS Institute, Cary, NC, USA).

RESULTS

Subject Characteristics

The characteristics of the study subjects are outlined in Table 1. Subjects ranged in age from 18 to 84 years old (mean age 48), with 157 (48%) females, and a mean MAP of 93 mm Hg. The majority of the cohort were White with smaller groups of Asian, Black, and Hispanic subjects, respectively.

Table 1. Cohort demographics

	Age groups (years old)			
	All subjects	*18–40*	*41–60*	*>60*
n	325	122	130	73
Mean age	48 ± 15	31 ± 6	51 ± 6	69 ± 6
Gender M/F (%M/%F)	52/48	56/44	43/57	60/40
Mean weight (kg)	75 ± 16	73 ± 16	76 ± 16	77 ± 14
Mean height (cm)	171 ± 10	171 ± 10	171 ± 10	170 ± 9
Mean MAP (mm Hg)	93 ± 11	88 ± 10	93 ± 10	100 ± 8
Race (%)				
Asian	72 (21)	28 (23)	26 (20)	18 (25)
Black	32 (10)	12 (10)	20 (15)	0 (0)
Hispanic	12 (4)	8 (7)	3 (2)	1 (1)
White	209 (64)	74 (61)	81(62)	54 (74)

F, female; M, male; MAP, mean arterial pressure. Age, weight and height are presented as mean ± 1 s.d.

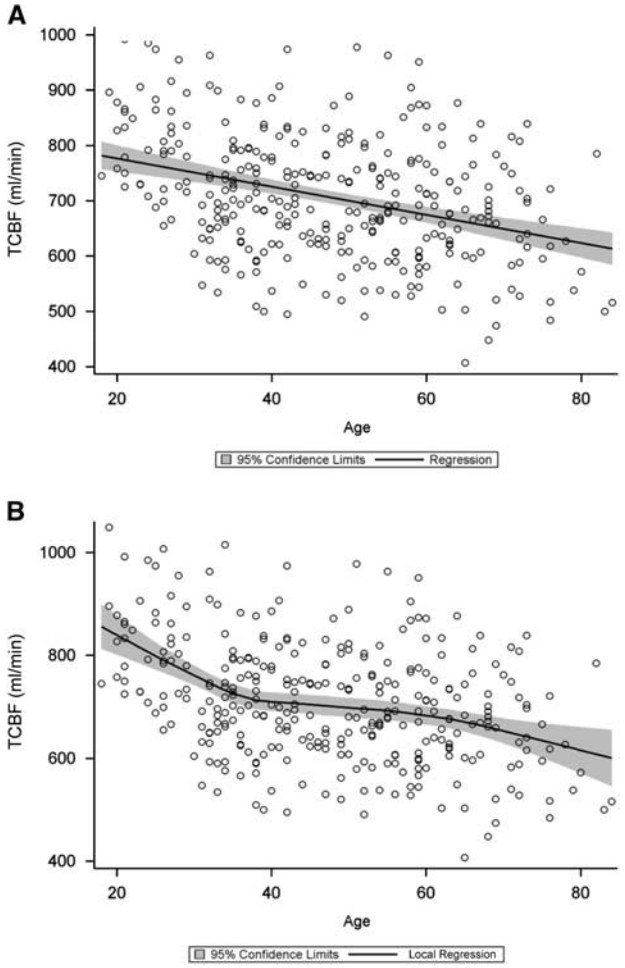

Figure 2. (**A**) TCBF (mL/minute) decrease with age in a linear regression model. (**B**) In a local regression model, there is a relative plateau in flow change in the mid-decades. TCBF, total cerebral blood flow.

Vessel Flow Rates and Age

Total CBF declined with age ($P < 0.001$) from 749 ± 115 mL/minute in the youngest decades (age 18 to 40 years) to 656 ± 103 mL/minute in the oldest decades (>60 years old), representing an average 2.6 mL/minute per year drop in a linear regression model (Figure 2A). However, examining the flow in a local regression model supported three distinct age groupings, with a relative plateau in flows in the mid-decades, from age 40 to 60 years (Figure 2B). On the basis of this observation, flows were categorized into three groups for ages 18 to 40, 41 to 60, and >60 years old (Table 2), and demonstrated a significant difference in individual vessel, and total, flows among the age groupings.

Table 2. Vessel flow rates

	All (CV%)	*18–40 y.o. (CV%)*	*41–60 y.o. (CV%)*	*61–80 y.o. (CV%)*	P-*value**
TCBF (*n* = 320)	706 ± 111 (16)	749 ± 115 (15)	700 ± 107 (15)	656 ± 103 (16)	< 0.01
Proximal arteries					
LCCA (*n* = 320)	392 ± 72 (18)	422 ± 75 (18)	382 ± 68 (18)	368 ± 73 (20)	< 0.01
RCCA (*n* = 315)	389 ± 75 (19)	407 ± 79 (19)	389 ± 68 (17)	369 ± 76 (21)	< 0.01
LICA (*n* = 320)	259 ± 50 (20)	273 ± 46 (17)	255 ± 51 (20)	243 ± 53 (22)	< 0.01
RICA (*n* = 320)	256 ± 52 (20)	267 ± 52 (19)	257 ± 49 (19)	235 ± 53 (22)	< 0.01
TVA (*n* = 323)	190 ± 45 (24)	201 ± 46 (23)	187 ± 42 (22)	175 ± 41 (23)	< 0.01
LVA (*n* = 323)	100 ± 38 (38)	110 ± 38 (35)	97 ± 37 (38)	88 ± 37 (42)	< 0.01
RVA (*n* = 315)	88 ± 30 (34)	89 ± 31 (35)	89 ± 25 (28)	87 ± 33 (38)	0.65
BA (*n* = 323)	138 ± 41 (30)	149 ± 44 (30)	137 ± 41 (30)	124 ± 31 (25)	< 0.01
Distal arteries					
LMCA (*n* = 315)	159 ± 28 (18)	170 ± 33 (20)	159 ± 27 (17)	146 ± 22 (15)	< 0.01
RMCA (*n* = 319)	146 ± 28 (19)	159 ± 31 (19)	144 ± 24 (17)	133 ± 26 (19)	< 0.01
LPCA (n = 318)	69 ± 14 (21)	72 ± 14 (19)	68 ± 12 (18)	61 ± 12 (20)	< 0.01
RPCA (*n* = 318)	66 ± 15 (22)	72 ± 16 (22)	65 ± 14 (21)	58 ± 12 (21)	< 0.01
TACA (*n* = 308)	175 ± 35 (20)	188 ± 38 (20)	171 ± 31 (18)	160 ± 32 (18)	< 0.01
LACA (*n* = 318)	86 ± 26 (31)	94 ± 26 (27)	80 ± 23 (29)	79 ± 26 (33)	< 0.01
RACA (*n* = 307)	93 ± 28 (30)	96 ± 32 (33)	94 ± 26 (28)	86 ± 32 (37)	0.08
LA2 (*n* = 190)	74 ± 18 (25)	82 ± 16 (19)	68 ± 14 (21)	70 ± 18 (25)	< 0.01
RA2 (*n* = 187)	72 ± 15 (21)	78 ± 14 (19)	70 ± 13 (19)	68 ± 15 (23)	< 0.01
Regional flow					
LR (*n* = 188)	304 ± 50 (17)	337 ± 48 (14)	300 ± 42 (14)	280 ± 50 (18)	< 0.01
RR (*n* = 191)	285 ± 53 (19)	326 ± 54 (17)	279 ± 43 (16)	258 ± 45 (18)	< 0.01
PR (*n* = 321)	273 ± 61 (22)	326 ± 54 (17)	279 ± 43 (16)	255 ± 42 (17)	< 0.01

A2, ACA post-communicating segment; ACA, anterior cerebral artery; BA, basilar artery; CCA, common carotid artery; CV, coefficient of variation; ICA, internal carotid artery; L, left; MCA, middle cerebral artery; *n*, sample size (reflects exclusion of outliers); PCA, posterior cerebral artery; PR, posterior region; R, right; T, total; TCBF, total cerebral blood flow; VA, vertebral artery; y.o., years old. Flow rates in mL/minute ± 1 s.d. in the major cerebral vessels. **P*-value for differences between age groups.

Table 3. Vessel flow indices in representative vessels

	All (CV%)	*18–40 y.o. (CV%)*	*41–60 y.o. (CV%)*	*61–84 y.o. (CV%)*	P-*value**
Proximal arteries					
LICA (*n* = 309)	0.37 ± 0.04 (11)	0.37 ± 0.04 (10)	0.36 ± 0.04 (12)	0.37 ± 0.04 (11)	0.55
RICA (*n* = 312)	0.36 ± 0.04 (12)	0.36 ± 0.04 (12)	0.37 ± 0.04 (11)	0.36 ± 0.05 (15)	0.28
TVA (*n* = 319)	0.27 ± 0.04 (17)	0.27 ± 0.04 (16)	0.27 ± 0.05 (17)	0.28 ± 0.04 (14)	0.50
BA (*n* = 311)	0.20 ± 0.04 (21)	0.20 ± 0.04 (18)	0.20 ± 0.05 (24)	0.20 ± 0.04 (21)	0.34
Distal arteries					
LMCA (*n* = 315)	0.23 ± 0.02 (11)	0.23 ± 0.03 (11)	0.23 ± 0.02 (10)	0.22 ± 0.02 (9)	0.34
RMCA (*n* = 316)	0.21 ± 0.02 (12)	0.21 ± 0.02 (12)	0.21 ± 0.02 (11)	0.20 ± 0.02 (11)	0.03
LPCA (*n* = 314)	0.10 ± 0.02 (16)	0.10 ± 0.02 (19)	0.10 ± 0.01 (15)	0.09 ± 0.01 (13)	0.06
RPCA (*n* = 308)	0.09 ± 0.01 (15)	0.10 ± 0.02 (18)	0.09 ± 0.01 (12)	0.09 ± 0.01 (13)	0.01
TACA (*n* = 298)	0.25 ± 0.03 (12)	0.25 ± 0.03 (12)	0.25 ± 0.03 (13)	0.25 ± 0.03 (12)	0.26
LA2 (*n* = 180)	0.10 ± 0.02 (18)	0.10 ± 0.02 (15)	0.10 ± 0.02 (19)	0.11 ± 0.02 (19)	0.32
RA2 (*n* = 185)	0.10 ± 0.02 (16)	0.10 ± 0.02 (18)	0.10 ± 0.01 (14)	0.11 ± 0.02 (17)	0.19
Regional flow					
LR (*n* = 185)	0.43 ± 0.04 (8)	0.44 ± 0.04 (8)	0.43 ± 0.03 (8)	0.42 ± 0.03 (8)	0.03
RR (*n* = 180)	0.40 ± 0.03 (8)	0.41 ± 0.03 (6)	0.40 ± 0.04 (9)	0.40 ± 0.03 (8)	0.14
PR (*n* = 316)	0.39 ± 0.06 (15)	0.40 ± 0.06 (15)	0.38 ± 0.06 (15)	0.38 ± 0.05 (13)	0.06

A2, ACA post-communicating segment; ACA, anterior cerebral artery; BA, basilar artery; CV, coefficient of variation; ICA, internal carotid artery; L, left; MCA, middle cerebral artery; *n*, sample size (reflects exclusion of outliers); PCA, posterior cerebral artery; PR, posterior region; R, right; T, total; VA, vertebral artery; y.o., years old. Indices: individual vessel flows in mL/minute per total cerebral blood flow (TCBF) in mL/minute. **P*-value for differences between age groups.

Although age grouping provide more accurate age-relevant reference ranges for vessel flow, variability as reflected in the coefficient of variation (CV) remains high (Table 2), making their use as reference values less practical. To adjust for the flow variability introduced by the effect of age, individual vessel flows were indexed to TCBF. In so doing, TCBF-adjusted flow indices were generated for each major cerebral vessel, which were largely effective in neutralizing the age effect and reducing the CV within the reference ranges (Table 3). This allows designation of normative percentiles thresholds for vessel-specific flow index, irrespective of a subject's age (Supplementary Table).

Vessel Flow Rates and Systemic Variables

On univariate analysis, TCBF did not demonstrate any relationship relative to sex or race, but was negatively associated with MAP ($P < 0.01$). However, on multivariate analysis adjusting for age, flow was not found to be significantly altered through the MAP range ($P = 0.37$).

Vessel Flow Rates and Vascular Anatomy

For paired vessels, only the LMCA and LPCA demonstrated significantly higher flows than their R-sided counterpart ($P < 0.01$). Vessels proximal to the Circle of Willis, namely the ICAs and BA were examined relative to anatomic variants within the Circle: fetal PCA, hypoplastic/absent PCoA, and hypoplastic/absent A1 segment of the ACA. Flows relative to these anatomic variants are summarized in Table 4. Although BA flow in the overall cohort averaged 138 ± 41 mL/minute, flow was significantly decreased in subjects with one or both fetal PCAs (84 ± 27 mL/minute) compared with those with no PCoAs (156 ± 31 mL/minute; $P < 0.01$; Figure 3A). Similarly, ICA flows were affected by PCoA and PCA anatomy (Figure 3B), being significantly higher on the side of a fetal PCA (278 ± 55 mL/minute) compared with on the side of an absent PCoA (248 ± 50 mL/minute; $P < 0.01$). The ICA flow was also impacted by the A1 segment anatomy; flow was significantly decreased in the setting of an ipsilateral absent or hypoplastic A1 segment at 194 ± 49 mL/minute compared with 258 ± 50 mL/minute ($P < 0.01$) in the setting of a normal A1 (Figure 3C).

The variability introduced by these anatomic variations is evident in the wider CVs for some of the proximal vessels (VAs: 34% to 38%; BA: 30%) as compared with the more distal terminal vessels (MCA: 18% to 19%, A2s: 21% to 25% and PCA: 21% to 22%; Table 2). These relative differentials persist even when considering flow indices rather than absolute flow in these individual vessels (Table 3). Variability is reduced most by examining flow indices in regional flow reflecting the posterior circulation as a whole (PR:15%) or hemispheric flow (LR and RR: 8%).

DISCUSSION

The feasibility of blood flow measurements in individual cerebral vessels using phase contrast QMRA has been previously well demonstrated.[13,14] Such information can be of significant clinical benefit in evaluating disease states affecting the cerebral vasculature, such as atherosclerotic occlusive disease, moyamoya, and arteriovenous malformations.[2,15–18] However, paramount to interpreting flow information in disease states is the understanding of

Table 4. Flow and indices in proximal vessels relative to common anatomic variants

	All	*18–40 y.o.*	*41–60 y.o.*	*61–84 y.o.*	P-*value*
ICA					
Fetal PCA (n = *48*)					
Flow	278 ± 55	284 ± 62	282 ± 50	261 ± 48	0.52
Index	0.41 ± 0.05	0.40 ± 0.05	0.43 ± 0.03	0.40 ± 0.05	0.15
PCoA (non-fetal) (n = *260*)					
Flow	264 ± 50	275 ± 49	258 ± 46	253 ± 56	0.01
Index	0.37 ± 0.04	0.37 ± 0.04	0.37 ± 0.04	0.37 ± 0.05	0.87
No PCoA (n = *331*)					
Flow	248 ± 50	263 ± 47	250 ± 50	229 ± 50	< 0.01
Index	0.35 ± 0.03	0.35 ± 0.03	0.35 ± 0.03	0.35 ± 0.05	0.55
Ipsilateral hypolastic A1 (n = *17*)					
Flow	194 ± 49	228 ± 55	206 ± 46	165 ± 37	0.10
Index	0.29 ± 0.05	0.32 ± 0.06	0.31 ± 0.05	0.26 ± 0.04	0.10
Normal A1[a] (n = *606*)					
Flow	258 ± 50	270 ± 48	256 ± 49	241 ± 50	< 0.01
Index	0.36 ± 0.04	0.36 ± 0.04	0.36 ± 0.04	0.36 ± 0.04	0.98
Contralateral hypolastic A1 (n = *17*)					
Flow	293 ± 38	311 ± 42	285 ± 35	276 ± 24	0.30
Index	0.45 ± 0.04	0.44 ± 0.07	0.44 ± 0.01	0.46 ± 0.04	0.59
BA					
Fetal PCA[b] (n = *40*)					
Flow	84 ± 27	91 ± 29	76 ± 23	85 ± 30	0.32
Index	0.13 ± 0.04	0.13 ± 0.04	0.12 ± 0.04	0.14 ± 0.01	0.25
PCoA (non-fetal)[c] (n = *169*)					
Flow	139 ± 39	153 ± 43	137 ± 37	121 ± 33	< 0.01
Index	0.20 ± 0.04	0.20 ± 0.03	0.19 ± 0.04	0.18 ± 0.04	0.02
No PCoAs (n = *114*)					
Flow	156 ± 31	169 ± 25	157 ± 31	141 ± 30	< 0.01
Index	0.22 ± 0.03	0.22 ± 0.02	0.22 ± 0.03	0.22 ± 0.03	0.82

A1, anterior cerebral artery proximal pre-communicating segment; BA, basilar artery; ICA, internal carotid artery; *n*, sample size (reflects exclusion of outliers); PCA, posterior cerebral artery; PCoA, posterior communicating artery; y.o., years old. Flow rates in mL/minute ± 1 s.d. Indices: individual vessel flows in mL/minute per total cerebral blood flow (TCBF) in mL/minute. *P*-value for differences between age groups. [a]Nonhypoplastic A1 in the absence of contralateral hypoplasia. [b]Unilateral or bilateral fetal PCA. [c]PCoA present on one or both sides without fetal PCA.

normal cerebral vessel flows in the absence of cerebrovascular disease. In this study, we have measured major cerebral vessel flows in the largest cohort to date of healthy individuals spanning a broad adult age range, and have affirmed the effects of age and vascular anatomy on vessel flows. In addition, we have been able to demonstrate strategies to mitigate these effects, which serve as sources of variability in flow measurement: individual vessel flows can be indexed to TCBF to neutralize the effect of age, and vessels distal to the Circle of Willis or regional can be examined to lessen the impact of vascular anatomic variants on more proximal vessel flows. The data presented provide a robust data set to establish normative reference values for eventual comparison with cerebrovascular disease states.

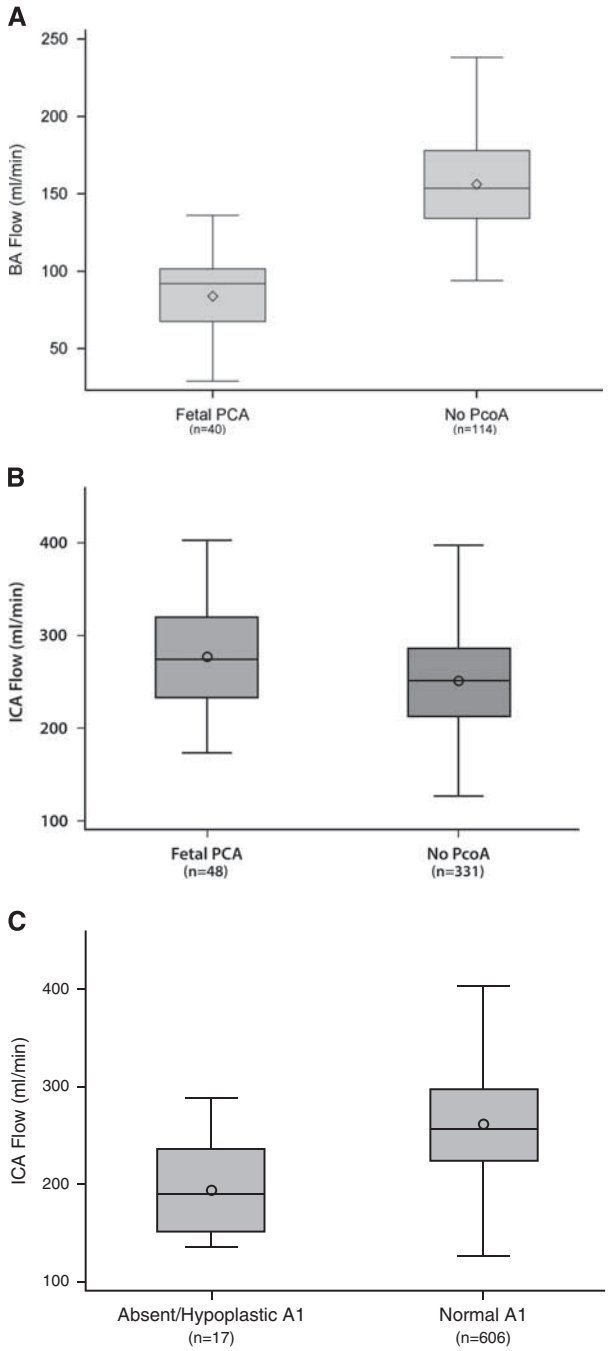

Figure 3. (**A**) Comparison of BA flow (mL/minute) relative to PCA and PCoA anatomy. (**B**) Comparison of ICA flow (mL/minute) relative to PCA and PCoA anatomy. (**C**) Comparison of ICA flow (mL/minute) relative to ACA A1 segment anatomy. A1, anterior cerebral artery proximal pre-communicating segment; ACA, anterior cerebral artery; BA, basilar artery; ICA, internal carotid artery; PCA, posterior cerebral artery; PCoA, posterior communicating artery.

The association we found between decreasing flow with age is comparable to prior reports.[8,10,19–21] Our data demonstrate an average overall 2.6 mL/minute per year change in flow, very similar to the 3.1 mL/minute per year decrease in total volume flow reported by Hendrikse *et al*[10] in their analysis of 208 patients with mean age of 60 (range 29 to 79). In their study, total volume flow was calculated on the basis of the sum of ICA and BA flow, as opposed to ICA and VA flow. Similarly, Buijs *et al*[8] calculated flow on the basis of ICA and BA flow in 250 patients ranging from 19 to 89 years old, and described a slightly higher 4.8 mL/minute per year average flow decline. It should be noted that the prior studies included not only healthy volunteers, but also patients with risk factors for atherosclerosis, which could potentially alter total flows, especially in the older age groups, and exaggerate the flow decline observed. Total cerebral flows averaged in the 610 to 620 mL/minute range in these prior studies with comparable sample size,[8,10] lower than the average TCBF of 698 mL/minute in our series; this can be attributed primarily to the use of VA rather than BA flow in calculating TCBF in our series, given that the BA flow (which was measured proximal to the origin of the superior cerebellar arteries in prior studies) only includes a portion of the cerebellar flow. However, average ICA flows across the studies are very similar, in the 240 to 260 mL/minute range, despite different populations at different centers, providing further validation of the consistency of cerebral vessel flow measurement with QMRA phase contrast technique. A larger study of 892 elderly subjects (not limited to healthy volunteers) with a mean age of 67.5 years old (range 60 to 92), not surprisingly, found lower TCBF and ICA flow values[22] averaging ~500 mL/minute and 200 mL/minute, respectively.

Gender differences in CBF have been reported by some,[21,22] whereas none have been found by others.[8,20,23] We did not detect a significant difference in flows between males and females, nor by race, although evaluation is limited by the small sample size in the various racial groups.

Our study is the first to have explicitly measured and examined the effects of blood pressure on measured flows. When adjusted for age, MAP was not found to affect vessel flows, consistent with the concepts of cerebral autoregulation. However, given these subjects were healthy volunteers, screened to avoid hypertensive history, the effect of chronic hypertension or extremes of blood pressure on cerebral vessel flow cannot be adequately evaluated in our cohort. Towards the edges of the physiologic autoregulatory curve, or in the setting of impaired autoregulation seen in chronic ischemic states, it might be expected for the vessel flow to change in response to blood pressure variations.

The effects we observed of fetal PCA and hypoplastic A1 anatomic variants on ICA and BA flow have also been evident in prior studies.[9,10] As in our cohort, both Hendrikse *et al*[10] and Tanaka *et al*[9] found a decreased ICA flow ipsilateral to a hypolastic A1, and elevated ICA flows contralateral because of the necessity to supply both ACA territories. Similarly in those studies, BA flow was found to be significantly reduced and ICA flow significantly increased in the setting of fetal PCAs. Such variants affected 17% of our cohort, and up to 25% of individuals may harbor such anatomic variants.[24,25] Thus, recognition of the impact of these variants in the Circle of Willis is critical to the interpretation of flow measured in the proximal intracranial vessels. We have additionally demonstrated in our cohort the reduction of variability in the more distal vessels, the MCA, A2, and PCA, by comparison, and in regional flows focused on hemispheric or posterior circulations. Regional flows provide the advantage of providing the full territorial flow to a hemisphere or region, incorporating both primary (Willisian) and secondary

(leptomeningeal) collaterals. In cerebrovascular occlusive disease, where collateral flow can compensate for flow reduction in an occluded or stenotic vessel,[26] regional flow may provide a more accurate and robust indication of overall flow compromise. Such interpretations would be limited, however, in conditions with blood supply from unmeasured sources, such as dural collaterals, e.g., moyamoya disease.

With our data we have also demonstrated that indexing a specific vessel flow to TCBF will largely adjust for the age effect otherwise encountered. This reflects the finding that the reduction in TCBF, which occurs with age is uniformly distributed across all vessels in healthy subjects, and thus the relative contribution of each vessel studied remains constant despite the increasing age. Care must be taken, however, in extrapolating reference values for vessel flow indices in cerebrovascular disease states, as the TCBF to which the flow is indexed could itself be altered by the disease, thus skewing the index towards normalcy. The utility of vessel indices as reference values for cerebrovascular disease will need to be further examined in future studies.

Limitations of our study include the lack of anatomic brain imaging suitable for determination of brain volumes. Thus, although the reduction in blood flow with age is presumed to be related to brain atrophy, we are not able to provide direct confirmation of this relationship. Furthermore, we similarly cannot definitively exclude the existence of potential asymptomatic vascular malformations, brain lesions, or infarcts, which may influence CBF, although the limited assessment of brain parenchyma visualized from the TOF source imaging did not grossly reveal such abnormalities. Furthermore, the study criteria were aimed at the recruitment of healthy subjects without major risk factors for, or existing, cerebrovascular disease. The possibility of other conditions, which could theoretically impact blood flow such as migraine history, however, cannot be excluded. Our data also represents a single center cohort, lacking the additional validation of a multi-site study; however, our flow data have consistency with flow rates measured in comparable vessels using QMRA techniques in other published series,[8,10] supporting the generalizability of our results.

CONCLUSION

In conclusion, we have demonstrated that volume flow rates in all major cerebral arteries can be obtained noninvasively using QMRA, and are influenced by age and vascular anatomy. The data represent the largest set of reference values for a comprehensive set of cerebral vessels in healthy subjects across a clinically useful age range. Knowledge of the expected normal vessel flows, incorporating patient-specific age and accounting for anatomy, are critical to interpreting the hemodynamic effects of cerebrovascular disease states.

DISCLOSURE/CONFLICT OF INTEREST

SAH receives material research support (no direct funds) from GE Healthcare and VasSol; FTC has financial interest in VasSol. The remaining authors declare no conflict of interest.

REFERENCES

1 Derdeyn CP, Grubb RL, Jr, Powers WJ. Cerebral hemodynamic impairment: methods of measurement and association with stroke risk. *Neurology* 1999; **53**: 251–259.
2 Amin-Hanjani S, Du X, Zhao M, Walsh K, Malisch TW, Charbel FT. Use of quantitative magnetic resonance angiography to stratify stroke risk in symptomatic vertebrobasilar disease. *Stroke* 2005; **36**: 1140–1145.
3 Amin-Hanjani S, Shin JH, Zhao M, Du X, Charbel FT. Evaluation of extracranial-intracranial bypass using quantitative magnetic resonance angiography. *J Neurosurg* 2007; **106**: 291–298.
4 Hendrikse J, van der Zwan A, Ramos LM, Tulleken CA, van der Grond J. Hemodynamic compensation via an excimer laser-assisted, high-flow bypass before and after therapeutic occlusion of the internal carotid artery. *Neurosurgery* 2003; **53**: 858–863.
5 Hendrikse J, Rutgers DR, Klijn CJ, Eikelboom BC, van der Grond J. Effect of carotid endarterectomy on primary collateral blood flow in patients with severe carotid artery lesions. *Stroke* 2003; **34**: 1650–1654.
6 Amin-Hanjani S, Alaraj A, Calderon-Arnulphi M, Aletich VA, Thulborn KR, Charbel FT. Detection of intracranial in-stent restenosis using quantitative magnetic resonance angiography. *Stroke* 2010; **41**: 2534–2538.
7 Prabhakaran S, Wells KR, Jhaveri MD, Lopes DK. Hemodynamic changes following wingspan stent placement--a quantitative magnetic resonance angiography study. *J Neuroimaging* 2011; **21**: e109–e113.
8 Buijs PC, Krabbe-Hartkamp MJ, Bakker CJ, de Lange EE, Ramos LM, Breteler MM *et al.* Effect of age on cerebral blood flow: measurement with ungated two-dimensional phase-contrast mr angiography in 250 adults. *Radiology* 1998; **209**: 667–674.
9 Tanaka H, Fujita N, Enoki T, Matsumoto K, Watanabe Y, Murase K *et al.* Relationship between variations in the circle of Willis and flow rates in internal carotid and basilar arteries determined by means of magnetic resonance imaging with semiautomated lumen segmentation: reference data from 125 healthy volunteers. *AJNR Am J Neuroradiol* 2006; **27**: 1770–1775.
10 Hendrikse J, van Raamt AF, van der Graaf Y, Mali WP, van der Grond J. Distribution of cerebral blood flow in the circle of Willis. *Radiology* 2005; **235**: 184–189.
11 Zhao M, Charbel FT, Alperin N, Loth F, Clark ME. Improved phase-contrast flow quantification by three-dimensional vessel localization. *Magn Reson Imaging* 2000; **18**: 697–706.
12 Calderon-Arnulphi M, Amin-Hanjani S, Alaraj A, Zhao M, Du X, Ruland S *et al.* *In vivo* evaluation of quantitative MR angiography in a canine carotid artery stenosis model. *AJNR Am J Neuroradiol* 2011; **32**: 1552–1559.
13 Enzmann DR, Ross MR, Marks MP, Pelc NJ. Blood flow in major cerebral arteries measured by phase-contrast cine mr. *AJNR Am J Neuroradiol* 1994; **15**: 123–129.
14 Spilt A, Box FM, van der Geest RJ, Reiber JH, Kunz P, Kamper AM *et al.* Reproducibility of total cerebral blood flow measurements using phase contrast magnetic resonance imaging. *J Magn Reson Imaging* 2002; **16**: 1–5.
15 Guppy KH, Charbel FT, Corsten LA, Zhao M, Debrun G. Hemodynamic evaluation of basilar and vertebral artery angioplasty. *Neurosurgery* 2002; **51**: 327–333.
16 van Everdingen KJ, Klijn CJ, Kappelle LJ, Mali WP, van der Grond J. MRA flow quantification in patients with a symptomatic internal carotid artery occlusion. The Dutch EC-IC Bypass Study Group. *Stroke* 1997; **28**: 1595–1600.
17 Marks MP, Pelc NJ, Ross MR, Enzmann DR. Determination of cerebral blood flow with a phase-contrast cine MR imaging technique: evaluation of normal subjects and patients with arteriovenous malformations. *Radiology* 1992; **182**: 467–476.
18 Neff KW, Horn P, Schmiedek P, Duber C, Dinter DJ. 2D cine phase-contrast MRI for volume flow evaluation of the brain-supplying circulation in moyamoya disease. *AJR Am J Roentgenol* 2006; **187**: W107–W115.
19 Spilt A, Weverling-Rijnsburger AW, Middelkoop HA, van Der Flier WM, Gussekloo J, de Craen AJ *et al.* Late-onset dementia: structural brain damage and total cerebral blood flow. *Radiology* 2005; **236**: 990–995.
20 van Raamt AF, Appelman AP, Mali WP, van der Graaf Y. Arterial blood flow to the brain in patients with vascular disease: the SMART Study. *Radiology* 2006; **240**: 515–521.
21 Tarumi T, Ayaz Khan M, Liu J, Tseng BY, Parker R, Riley J *et al.* Cerebral hemodynamics in normal aging: central artery stiffness, wave reflection, and pressure pulsatility. *J Cereb Blood Flow Metab* 2014; **34**: 971–978.
22 Vernooij MW, van der Lugt A, Ikram MA, Wielopolski PA, Vrooman HA, Hofman A *et al.* Total cerebral blood flow and total brain perfusion in the general population: the Rotterdam Scan Study. *J Cereb Blood Flow Metab* 2008; **28**: 412–419.
23 Zhao M, Amin-Hanjani S, Ruland S, Curcio AP, Ostergren L, Charbel FT. Regional cerebral blood flow using quantitative MR angiography. *AJNR Am J Neuroradiol* 2007; **28**: 1470–1473.
24 Krabbe-Hartkamp MJ, van der Grond J, de Leeuw FE, de Groot JC, Algra A, Hillen B *et al.* Circle of Willis: Morphologic variation on three-dimensional time-of-flight MR angiograms. *Radiology* 1998; **207**: 103–111.
25 Jongen JC, Franke CL, Soeterboek AA, Versteege CW, Ramos LM, van Gijn J. Blood supply of the posterior cerebral artery by the carotid system on angiograms. *J Neurol* 2002; **249**: 455–460.
26 Ruland S, Ahmed A, Thomas K, Zhao M, Amin-Hanjani S, Du X *et al.* Leptomeningeal collateral volume flow assessed by quantitative magnetic resonance angiography in large-vessel cerebrovascular disease. *J Neuroimaging* 2009; **19**: 27–30.

Supplementary Information accompanies the paper on the Journal of Cerebral Blood Flow & Metabolism website (http://www.nature.com/jcbfm)